Journal of Mechanical Engineering Research and Developments
ISSN: 1024-1752
CODEN: JERDFO
Vol. 43, No.6, pp. 404-417
Published Year 2020

Numerical Investigation of Nanofluid in a Rectangular Microchannel Heat Sink

Wajeeh Kamal Hasan[†], Ameer Resan Kalash[‡], Hasanen Mohammed Hussen[‡†]

Laith Jaafer Habeeb[‡]

[†]Al-Rafidain University Collage / Refrigeration and Air Conditioning Engineering Department
[‡]University of Technology / Training and Workshop Center
[‡†]University of Technology / Mechanical Engineering Department

*Corresponding Author Email: laithhabeeb1974@gmail.com; dr.wajeeh21@gmail.com; Star.mero79@yahoo.com; hasanen.alsaady@yahoo.com

ABSTRACT: The heat transfer in a 3-D rectangular microchannel heat sink (MCHS) for single phase liquid flow using nanofluids is numerically investigated for laminar flow (Re = 60-700). In the present work, the performance of microchannel using CuO/H_2O nanofluid as a coolant with different volume concentrations ranged from 0 % to 5% is examined. The partial governing equations of fluid flow and heat are solved using ANSYS fluent 12.0 based on finite volume method. The evaluated microchannel performance was shown in terms of temperature and velocity contours, average Nusselt number and pressure drop. The thermo-physical properties of nanofluid are evaluated to study its effect on the flow and heat transfer at a reference bulk temperature. A Constant heat flux of 100W/cm^2 will be provided to the bottom side of highly conductive silicon substrate. The present CFD calculated wall temperature and friction factor values were associated with the analytical data and good agreement is detected. The results revealed that the nanofluids aid to improve the coefficient of heat transfer by 11% when CuO/H_2O nanofluid was used. The effect of the concentration of CuO nanofluid has been discussed with Reynolds number value and with the velocity of fluid. Furthermore, plots and calculations for the heat transfer coefficients and the average Nusselt number were carried out.

KEYWORDS: Nanofluid, Heat transfer enhancement, Forced Convection, Laminar flow.

INTRODUCTION

In the beginning of the seventies of this century, technology of micromachining had been employed to develop the heat sink because of its small dimensions and less coolant demands advantages. Microchannels are one of the most essential techniques, therefore the investigation of convective heat transfer and fluid flow in these devices is very important, because of the essential roles of such devices for engineering applications and medical problems. There are many studies focused on using nanofluid as a heat enhancer in microchannel:

Mohammed et al. [1] focused on characteristics of heat transfer and nanofluid laminar flow in rectangular MCHS under constant heat flux of 1000W/m^2. The effect of nanofluids on the heat transfer improvement at variant volume concentration was studied. The result revealed that the increase of particle volume fraction leads to decrease the MCHS wall temperature. Lower particle volume fractions are more useful to enhance the heat transfer than of □ = 5% of Al_2O_3 / H_2O nanofluids. The increase of Reynolds number leads to an increase in the pressure drop along the microchannel. The presence of the nanoparticles in water enhances heat transfer coefficient as compared to pure water with a slight rise in the values of friction factor.

Bhattacharya et al. [2] studied numerically the flow and characteristics of heat of laminar flow in microchannel heat sink using Al_2O_3/H_2O nanofluid. They observed that the use of nanofluid augments the performance of microchannel as a result of decreasing fin thermal resistance of MCHS. They also observed that increasing the concentration of nanoparticles leads to an increase in the heat transfer rate, which is associated with the increase in pumping power that somewhat offsets the beneficial influence of employing nanofluid.

Wang et al. [3] conducted experimental study for evaluation of forced convective heat transfer and fluid flow in a rectangular microchannels using water methanol flowing through microchannels as a working fluid under laminar and transition condition. They discovered that the behavior of heat transfer on microchannels are very complex and influenced by the liquid velocity, fluid flow temperature and the size of microchannel.

Jung et al. [4] investigated experimentally the heat transfer coefficients and friction factor in a rectangular microchannel using Al_2O_3 nanofluid under laminar flow. The base fluid has been used during the experiment is a mixture of ethylene glycol and water with volume concentration of 1.8. They found that the coefficient of convective heat transfer was increasing as compared to base fluid with little friction loss. They also observed that the rising in Reynolds number leads to considerable rise in Nusselt number value, which is contradictory to the data from the conventional analysis.

Qu and Mudawar [5] implemented experimental and numerical study of heat transfer and pressure drop characteristics in a rectangular microchannel heat sink with dimensions (231 μm by 713 μm) under laminar flow regime. The cooling fluid that was used during the experiment is deionized water under constant heat flux with two levels, 100 W/cm^2 and 200 W/cm^2. The result show that for bottom wall of the channel, much higher heat flux and Nusselt number values are encountered near the channel inlet. The simulated data was validated with experimental results and outstanding agreement was found between them.

Mishan et al. [6] conducted experimental work to evaluate the characteristic of fluid flow and heat transfer and in a rectangular microchannel using water as a working fluid. The experiment revealed that, with taking the entrance influences, the traditional theory for water flow through microchannels is applicable. New technique was developed during the experiment to calculate temperature distribution of fluid inside the microchannel.

Ergu et al. [7] implemented experimental study to find the pressure drop and local mass transfer in a rectangular microchannel (length of 35 mm, width of 3.70 mm and height of 0.107 mm) using water as working fluid under laminar floe regime (Re = 100 – 845). The pressure drop was measured within the range mentioned by Reynolds number, while mass transfer was measured with a chemical solution at (Re=18–552) using the technique of electrochemical limiting diffusion current (ELDCT). They found that there was a good rapprochement between the experimental and theoretical correlation data of friction factors values. The Sherwood number correlation was also obtained.

Papautsky et al. [8] studied experimentally the influence of aspect ratio on friction constant in a rectangular microchannel under laminar flow regime using water as working fluid. The results showed that there is a rise of approximately 20% in the friction constant for a specified driving potential as compared to micro-scale predictions from the theory of Navier-Stokes. They discovered also at lower aspect ratio there is an increase in friction constant about 20%. A similar increase in friction constant was observed at Reynolds numbers less than 100.

Harms et al. [9] investigated the forced convective heat transfer and fluid flow in a rectangular microchannels with dimensions (251 μm width and 1000 μm depth) using of water under laminar flow condition. They found that, the measured local Nusselt number values agreed well with theory of classical developing-flow. **Koo and Kleinstreuer** [10] simulated numerically the conjugate heat transfer and fluid flow characteristics in a rectangular microchannel heat sink using two types of nanofluids CuO/water and CuO/EG. A new model has been used to calculate the dynamic viscosity and thermal conductivity of nanofluids. They discovered that the high aspect ratio is more desirable and the employment of large value of thermal conductivity nanoparticles results in improved results.

Kosar [11] investigated numerically the material substrate and thickness influence on the heat transfer and fluid flow in rectangular microchannel heat sink using water as working fluid. He discovered that microchannels that were fabricated from low thermal conductivity materials is low as compared with microchannel made from materials of high thermal conductivity. He also found that the Nusselt number in a thick substrate is little compared to the thin substrate configuration. **Mohammed et al.** [12] studied numerically the influence of employing nanoparticles on fluid flow characteristics and heat transfer in a rectangular microchannel heat sink.

They observed that the addition of nanoparticles improves the microchannel heat sink cooling at optimum nanoparticles value and with extreme conditions of constant heat flux.

Fayadh et al. [13] numerically investigated the fluid flow inside rectangular microchannel heat exchanger using Al_2O_3/water nanofluids under constant heat flux supplied at the bottom surface. ANSYS fluent was used as a CFD solver with volume of fraction ranging from 1-5% and nanoparticles with grain size (50 nm). The fluid flow in laminar region at (Re = 500-2000). During the simulation, heat transfer coefficients, drop of pressure, friction factor and pumping power were calculated. The simulated data revealed that increasing nanoparticles concentration leads to rising in the coefficient of the convective heat transfer and decrease the thermal resistance. The friction factor also increased with volume of fraction increase.

Srivastava et al. [14] the influence of cavities and ribs on heat transfer and flow characteristics was studied computationally. microchannel heat sink with convergent-divergent (CD) shape was investigated with diverse Reynolds number and constant heat flux. The overall thermal resistance was found to be decrease by adding cavities and ribs to the CD shape, moreover the heat transfer was enhanced by rising Reynolds number. **Mukherjee et al.** [15] a rectangular microchannel heat sink was studied using ZnO-Water, and TiO2-water nanofluids. High thermal conductive material was used to make the heat sink, thus superior cooling performance was showed by the Heat sink. The highest performance for cooling was found by using nanofluids over pure water.

Saravanan et al. [16] microchannel pin fin heat sink was compared with the micro pin fin heat sink , characteristics of heat transfer and fluid flow was investigated numerically. Divers values of Reynolds number and constant heat flux was used for this simulations. the results illustrated that the highest values of friction factor and Nusselt number was calculated by using Micro channel pin fin heat sink. However the best thermal performance was found using pin fin heat sink. **Mehrabi et al.** [17] investigated the hydraulic and thermal enactment of a plate-pin fin heat sink. Experimental data was used to validate the numerical simulation results. Higher values of pressure drop and smaller values of thermal performance was found using a larger pin.

Ajeel et al. [18] numerically investigated a semicircle zigzag corrugated channel by studying the characteristics of thermal and hydraulic turbulent nanofluid flow. They found an enhancement in the thermal performance by using a zigzag profile of semicircle corrugated channel. In addition as the diameter of the nanoparticles increase the Nusselt number (Nu) decreases, however the (Nu) increase as the Reynolds number and the nanoparticles volume fraction rises. In this study, a computational unit cell will be modeled and a uniform heat flux of 100 W/cm^2 will be supplied to a highly conductive silicon bottom with the use of symmetrical property of the heat sink, also the influence of parameters such as Reynolds number and nanoparticles concentration on the improvement of nanofluids heat transfer will be studied.

MATHEMATICAL MODELING

Model Description

The model description of microchannel heat sink is shown in figure (1) and (2). Flowing nanofluid through a number of microchannels leads to removal of the heat supplied to the microchannel heat sink at a bottom surface of the duct, while the top surface of microchannel is subjected to adiabatic conditions. Considering a steady state fluid flowing through a rectangular shape of constant cross-section, the height and width of a rectangular microchannel are 180μm and 57μm respectively. Because of the symmetrical geometry and boundary conditions, thermal fields and flow are assumed to be symmetrical with respect to the vertical plane passing through the channel main axis, therefore, a half computational domain is considered. The fluid is exhausted into the ambient atmosphere which is at a pressure of (1) atm. The top surface and sides are assumed insulated except for the bottom side. The inlet temperature of fluid to the channel (T_{in}= 20^{o}C).

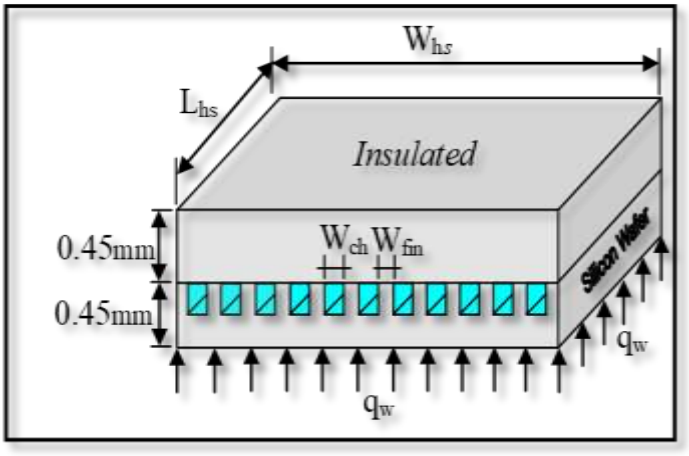

Figure 1. Structure of microchannel heat sink.

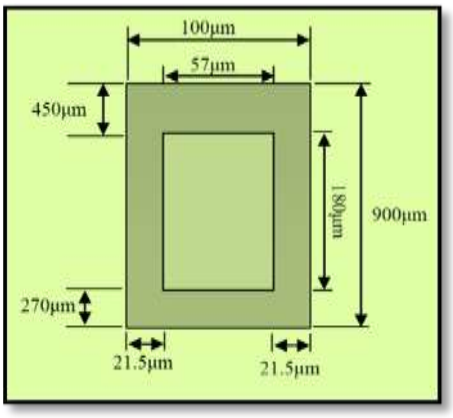

Figure 2. Isometric view of a section of a parallel microchannel array.

Thermal Properties of Nanofluids

Density and Viscosity

The effective density of the nanofluid containing suspended particles can be evaluated from the equation shown below:

$$\rho_{nf} = \left(\frac{m}{V}\right)_{nf} = \frac{m_{bf} + m_p}{V_{bf} + V_p} = \frac{\rho_{bf} V_{bf} + \rho_p V_p}{V_{bf} + V_p} = (1-\phi)\rho_{bf} + \phi\rho_p \quad \text{.....(1)}$$

Nguyen et al. [19] proposed an empirical correlation for CuO/water nanofluid and they derived from experimental data:

$$\mu_{nf} = \left(0.009\phi^3 + 0.051\phi^2 - 0.319\phi + 1.475\right)\mu_{bf} \quad \text{.....(2)}$$

Specific Heat

The specific heat of nanofluid can be determined by assuming thermal equilibrium between the nanoparticles and the base fluid phase as follows:

$$Cp_{nf} = \frac{(1-\phi)\rho_f Cp_f + \phi\rho_p Cp_p}{\rho_{nf}} \quad \text{.....(3)}$$

Thermal Conductivity Models

Mintsa et al. [20] based on his experimental data (table 1) proposed a model for CuO/water nanofluid:

$$k_{nf} = k_{bf}(1.74\phi + 0.99) \quad \text{.....(4)}$$

Table 1. Nanofluid properties with diverse CuO concentration

properties	ϕ **=0%**	ϕ **=2%**	ϕ **=5%**
$C_{p,\,nf}$ (J/kg K)	4182	3782.11	3311.87
μ_{nf} (Kg/m.s)	0.001002	0.001115	0.002285
ρ_{nf} (kg/m^3)	998.2	1108.24	1273.29
k_{nf} (W/m.K)	0.600	0.615	0.646

Numerical Simulation

Assumptions

The partial differential governing formals are continuity, Navier-Stoke's and energy equations are solved based on SIMPLE algorithm and the following assumptions have been taken into consideration:

❶ Three-dimensional and steady state conditions for heat transfer and fluid flow.
❷ Laminar flow, incompressible and single-phase fluid.
❸ Temperature independency for heat sink material properties and fluid.
❹ All heat sink walls are insulated except the bottom side of heat sink where constant heat flux and constant surface temperature boundary conditions simulating the heat generation from electronic chip is specified.
❺ The gravitational force and radiation heat transfer are negligible.

Governing Equations

Governing equations in single-phase model consists of continuity, Navier-Stoke's equations which are used for calculating velocity vector and energy equation, which is employed for calculating the wall heat transfer coefficient and temperature distribution. The simultaneous equations used for describing the case problem are:

Mass Conservation Equation

$$\frac{\partial u}{\partial x} + \frac{\partial v}{\partial y} + \frac{\partial w}{\partial z} = 0 \quad \text{.....(5)}$$

Momentum Conservation Equation

X-axis:

$$\rho_{nf}\left(u\frac{\partial u}{\partial x} + v\frac{\partial u}{\partial y} + w\frac{\partial u}{\partial z}\right) = -\frac{\partial p}{\partial x} + \mu_{nf}\left(\frac{\partial^2 u}{\partial x^2} + \frac{\partial^2 u}{\partial y^2} + \frac{\partial^2 u}{\partial z^2}\right) \quad \text{.....(6)}$$

Y-axis

$$\rho_{nf}\left(u\frac{\partial v}{\partial x} + v\frac{\partial v}{\partial y} + w\frac{\partial v}{\partial z}\right) = -\frac{\partial p}{\partial y} + \mu_{nf}\left(\frac{\partial^2 v}{\partial x^2} + \frac{\partial^2 v}{\partial y^2} + \frac{\partial^2 v}{\partial z^2}\right) \quad \text{.....(7)}$$

Z-axis

$$\rho_{nf}\left(u\frac{\partial w}{\partial x} + v\frac{\partial w}{\partial y} + w\frac{\partial w}{\partial z}\right) = -\frac{\partial p}{\partial z} + \mu_{nf}\left(\frac{\partial^2 w}{\partial x^2} + \frac{\partial^2 w}{\partial y^2} + \frac{\partial^2 w}{\partial z^2}\right) \quad \text{.....(8)}$$

Conservation of Energy

This equation is derived from the thermodynamics first law where the derivation of this law gives us the conservation of energy:

$$\rho C_p \frac{DT}{Dt} = k\nabla^2 T \quad \text{.....(9)}$$

The above energy equation can be divided into two several formals for both the solid mediums and the fluid as given by equations (3-7) and (3-6) respectively, if there is a steady conjugate heat transfer condition such as in combined conduction-convection problems.

$$(\rho C_p)_{nf}\left(u\frac{\partial T_{nf}}{\partial x}+v\frac{\partial T_{nf}}{\partial y}+w\frac{\partial T_{nf}}{\partial z}\right)=K_{nf}\left(\frac{\partial^2 T_{nf}}{\partial x^2}+\frac{\partial^2 T_{nf}}{\partial y^2}+\frac{\partial^2 T_{nf}}{\partial z^2}\right) \quad \text{.....(10)}$$

$$\frac{\partial}{\partial x}\left(K_s\frac{\partial T_s}{\partial x}\right)+\frac{\partial}{\partial y}\left(K_s\frac{\partial T_s}{\partial y}\right)+\frac{\partial}{\partial z}\left(K_s\frac{\partial T_s}{\partial z}\right)=0 \quad \text{.....(11)}$$

Boundary Conditions

For all internal surfaces, no slip boundary condition was considered (table 2). This means that the velocity components are zero ($u = \upsilon = 0$). Constant inlet temperature with uniform velocity were assumed at the channel inlet. Pressure was specified at channel exit. The top side of channel was adiabatic and the bottom side subjected to constant heat flux of 100W/cm^2. solid-fluid interfaces Coupled thermal boundary condition in this 3-D conjugate heat transfer problem was chosen. To avoid the need to explicitly specify heat flux or convective heat transfer factor at the interfaces between solid and fluid, the conjugate heat transfer was used. The fields of thermal and flow are considered symmetrical for the vertical plane, which pass into the channel longitudinal axis, this means that the gradient of all variables is zero [21].

Table 2. Boundary conditions of zone kind in ANSYS FLUENT.

Zone	**Wall**	**Left Sink**	**Bottom Sink**	**Top Sink**	**Outlet Sink**	**Inlet Sink**
Type	Wall	Wall	Wall	Wall	Wall	Wall

Zone	**Channel Left**	**Channel Right**	**Channel Bottom**	**Channel top**	**Channel Outlet**	**Channel Inlet**
Type	Wall	Wall	Wall	Wall	Out Flow	Inlet

Numerical Parameters and Mesh Generation

Finite Volume Method with hybrid differencing scheme have been used to solve the governing equations together with the boundary conditions and then the numerical calculations can be made. Fluid flow and solid equations were solved at the same time as a single problem [22] and then computational domain was initialized by guessing the field of pressure drop. It is very important to determine the velocity components by solving the momentum equation. The momentum and mass equations were not coupled to the energy equation because the buoyancy was neglected and it was assumed that the fluid had constant properties. Therefore, the temperature field was calculated by solving the energy equation after a converged solution for the flow field was obtained by solving the continuity and momentum.

Afterwards the continuity equation was transformed to correction equation to update the pressure. This procedure was continued until the residuals sum for all computational cells became less than 10^{-4} and components of velocity reached steady state and did not change with time during the iterations. A non-

uniform grid, which has been chosen, gave a precise accuracy as well as the consistency of numerical results, the chosen number of grid was sufficient for numerical results. The spacing among mesh cells is 2.5 μm in transverse direction and 100μm in flow direction. The total number of hexahedral cells in silicon zone are 635,000 and 100000 nanofluid fluid zone, as shown in figure (3). To discretize the momentum equations in three dimensions, a second order upwind scheme was employed. Convergence criteria were set to less than 1×10^{-4} for continuity and momentum residuals while set to less than 1×10^{-8} for energy.

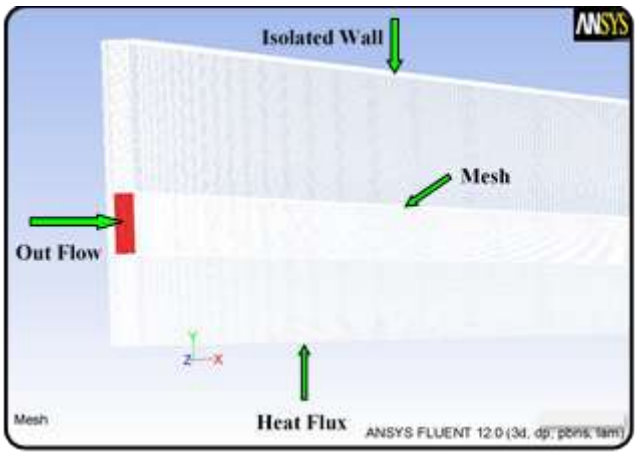

Figure 3. Geometry mesh raised view of a section.

SIMULATION RESULTS

Temperature Contours

The fluid temperature degree at the inlet is assumed constant at (20 ^{0}C). The temperature profiles were obtained based on hydrodynamic developed flow. It was noticed that the temperature at the corner of microchannel very high because of the low flow velocity, but at the channel exit is maximum. Figure (4) and (5) display the filled contours of temperature at outlet of the microchannel for pure water and CuO nanofluid, respectively. From examine the nanofluid has been used, the temperature at the outlet section increased because the fluid is heated up more due to the heat transfer by convection, which is clear from the temperature contour.

Velocity Contours

Figure (6) and (7) display the water velocity and its nanofluid at the outlet section for $\dot{m} = 1x10^{-5} kg/s$. When the pressure difference decreases gradually, the velocity decreases and the velocity increases towards the channel center. The velocity of the nanofluid at the center is less than that of pure water due to the particles weight, which lead to slow the flow rate.

Temperature Distribution Graphs

The large change in temperature degree towards the channel outlet at 100W/cm^2 power inputs along microchannel using water and nanofluids as the coolant are shown in figures (8) and (9), respectively. It can be observed that the use of pure water leads to more surface temperature than its nanofluids, and temperature of wall decreases with the increase in volume of fraction at a particular axial position. This affect occurs as the combined influence of density, thermal conductivity and viscosity.

Velocity Distribution Graph

The velocity distribution was used to study the hydrodynamics affect within the channel. The variation of velocity versus axial position (x) for water and its nanofluid are shown in figure (10). The figure illustrated that the required length to reach a fully developed flow is the same for all fluids. As the nanoparticles concentration increases in the base fluid, the viscosity and density of nanofluid increase and the velocity at any axial position decreases.

Pressure Drop and Friction factor Graph

It can be clearly observed that the pressure drop and friction factor increase with rising nanoparticles concentration at an equal Reynolds number as shown in figure (11), however, if a trial is made to increase *Re* value, an increase occurs in pressure drop, but friction factor decreases as can be seen below in table (3).

Table 3. Comparison of friction factor and computation drop of pressure of water and its nanofluids with analytical values.

Reynolds Number	**Computational value**		**Analytical value**	
	Friction Factor	Pressure Drop	Friction Factor	Pressure Drop
83.57	0.235	47.5	0.214	47.3
68.81	0.286	54.14	0.266	54.12
68.58	0.287	49.18	0.280	49.07
36.68	0.536	83.55	0.544	83.44

Nusselt Number Graph

From figure (12), the local Nusselt number keeps on decreasing toward the outlet at a particular heat flux due to the decrease in rate of convective heat transfer. Also, at a specified point in the microchannel, the local Nusselt number is different for different working fluid. It is also clear that the Nusselt number will be underestimated near the inlet and overestimated towards the outlet section and the results are similar to conventional results. The variations of the Nusselt number towards the exit are very small after the thermal entrance lengths for this type of microchannel heat sink.

Pumping Power Graph

The effect of nanofluid on the microchannel heat sink performance in terms of pumping power is shown in figure (13). It is very important to evaluate the nanofluids performance in terms of pumping power required to push the fluids along the channels. Pumping power is related to volumetric mass flow rates and pressure drop along the channels, and is given by [23]:

$$P_{pump} = \dot{V} \times \Delta P \quad \text{.....(12)}$$

It is observed that pumping power value increased with the increasing of volume of fraction, friction factor and number of channels, but it does not change with heat flux variation.

CONCLUSIONS

One type and design of microchannel was studied in this project. To understand the performance of microchannel cooling, variant boundary conditions and steady state cases were implemented using numerical simulation models. CFD code was used to solve the governing equations for the distribution of temperature and the velocity and results were shown in terms of the local Nusselt number and interface temperature. The parameters that were varied are Reynolds number and concentration of working fluid. The results showed that:

1. Due to the fact that the heat transfer coefficient for convection in locations in the upstream are greater as it has small boundary layer thickness, also due to the convective channel walls support downstream heat distribution, which means significant resistance from convection compared to the upstream parts of the channel, localized heat fluxes at small inlet regions of the microchannel under study are greater than fluxes at the downstream portion by two orders of magnitude.
2. Increasing Reynolds number values leads to an rise in Nusselt number and a decrease in the interface temperature, however, there is no considerable influence on the Nusselt number at the interface between fluid and solid.
3. The system thermal behavior was successfully represented by temperature contours.
4. The wall temperature of microchannel increases towards the outlet region.

5. Heat transfer coefficient increases as the volume of fraction increases. Greater value is obtained at entrance of microchannel. In general, the coefficient of heat transfer deceases from entry toward the exit of microchannel.

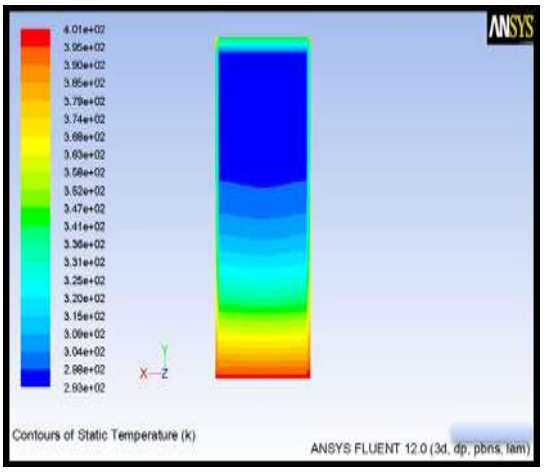

Figure 4. Temperature contour at the outlet of pure water at $\dot{m} = 1x10^{-5} kg/s$.

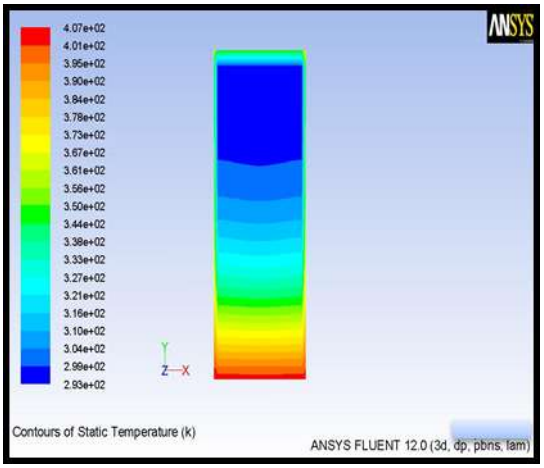

Figure 5. Temperature contour at the outlet of CuO nanofluid at $\dot{m} = 1x10^{-5} kg/s$.

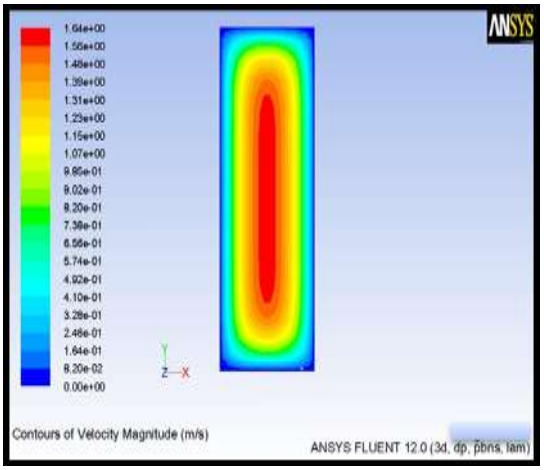

Figure 6. Velocity contour at the outlet of pure water at $\dot{m} = 1x10^{-5} kg/s$.

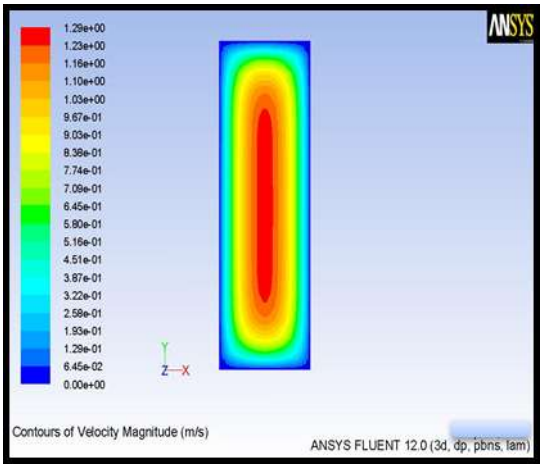

Figure 7. Velocity contour at the outlet of CuO nanofluid at $\dot{m} = 1x10^{-5} kg/s$.

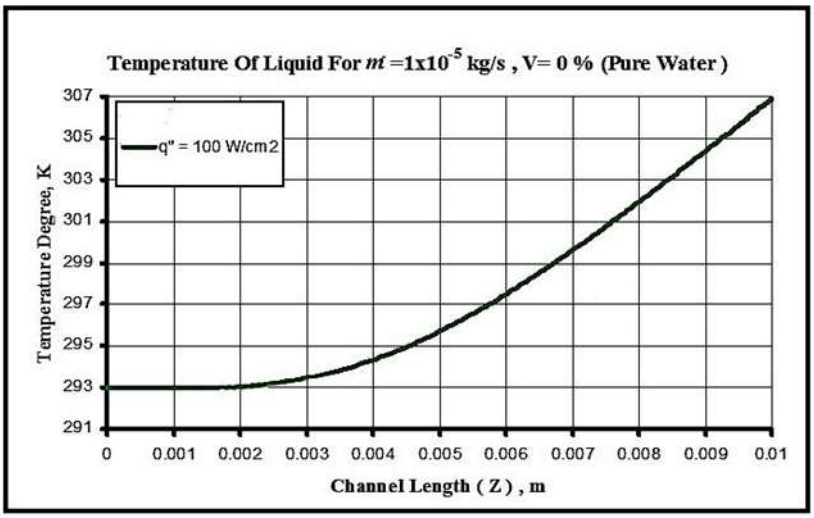

Figure 8. Variation on fluid temperature for (Re =83.57), (pure water).

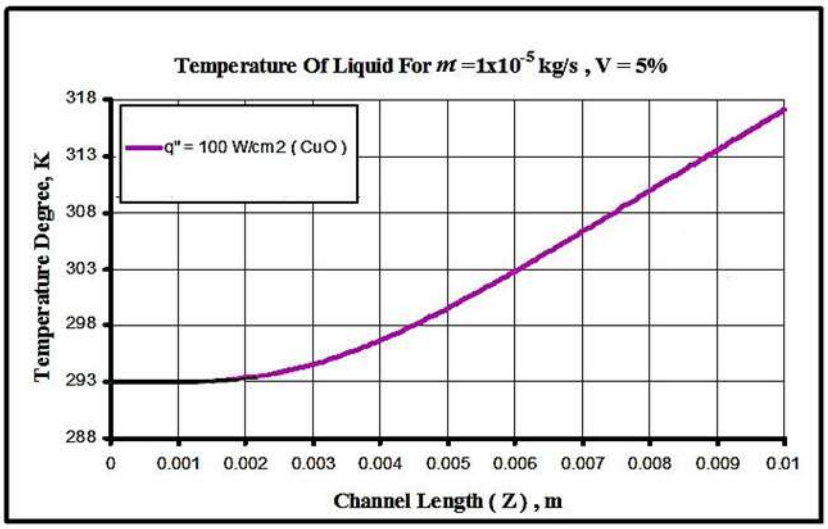

Figure 9. Variation on fluid temperature for (Re =83.57), (CuO nanofluid).

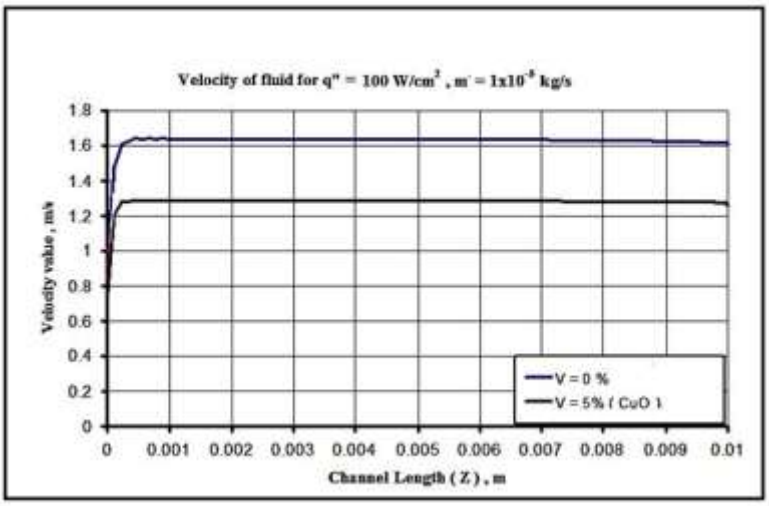

Figure 10. Nanofluid velocity profile at $\dot{m} = 1x10^{-5} kg/s$.

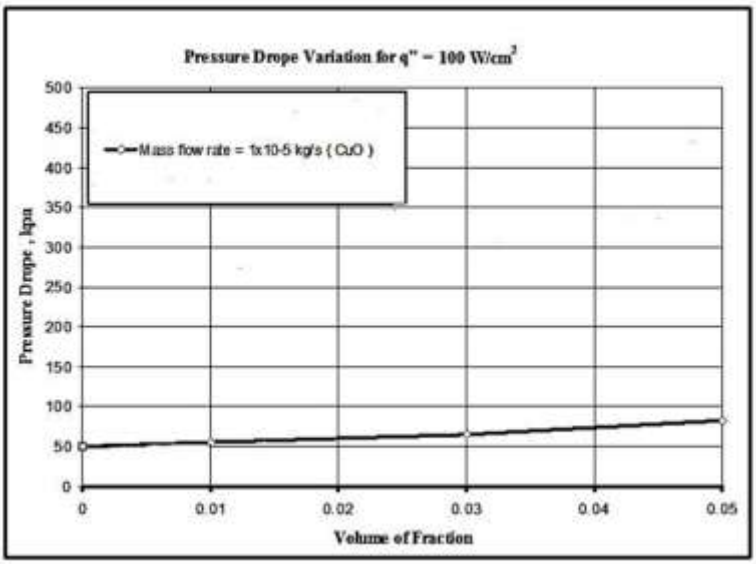

Figure 11. Variation of computational pressure at different concentration of CuO.

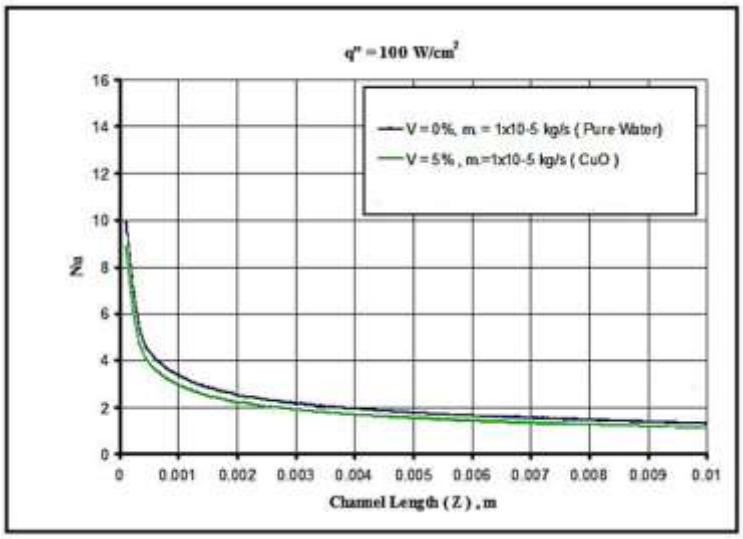

Figure 12. Nusselt number variation versus (Z) for different concentration at 100 W/cm^2.

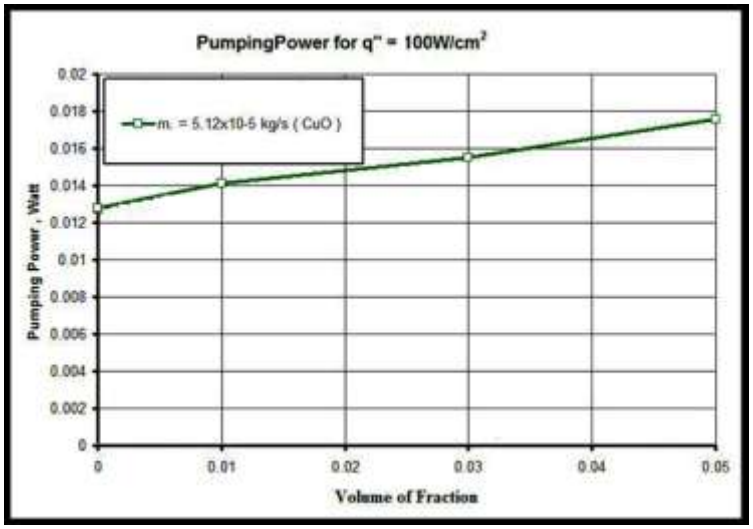

Figure 13. Pumping Power for q" = 100W/cm^2 and different volume concentration.

REFERENCES

[1] H.A. Mohammed, P. Gunnasegaran and N.H. Shuaib, "Heat transfer in rectangular microchannel heat sink using nanofluids", International Communications in Heat and Mass Transfer., Vol. 37, Pp. 1496 –1503, 2010.

[2] P. Bhattacharya, A.N. Samanta, and S. Chakraborty, "Numerical study of conjugate heat transfer in rectangular microchannel heat sink with Al_2O_3/H_2O nanofluid", 2009.

[3] B.X. Wang, X.F., Pucha, G.P. Peterson, and H.B. Ma, "Experimental investigation of heat transfer in flat plates with rectangular microchannels", International Journal of Heat and Mass Transfer, Vol. 38, No. 1, Pp. 127–137, 1995.

[4] J. Jung, H. Oh, and H. Kwak, "Forced convective heat transfer of Nanofluids in Microchannels", International Journal of Heat and Mass Transfer., Vol. 52, Pp. 466 – 472, 2009.

[5] W. Qu, and I. Mudawar, "Experimental and numerical study of pressure drop and heat transfer in a single-phase micro-channel heat sink", International Journal of Heat and Mass Transfer., Vol. 45, Pp. 2549 – 2565, 2002.

[6] Y. Mishan, A. Mosyak, E. Pogrebnyak, and G. Hetsroni, "Effect of developing flow and thermal regime on momentum and heat transfer in micro-scale heat sink", International Journal of Heat and Mass Transfer., Vol. 50, Pp. 3100 – 3114, 2007.

[7] O.B. Ergu, O.N. Sara, S. Yapıcı, and S. Arzutug, "Pressure drop and point mass transfer in a rectangular microchannel", International Communications in Heat and Mass Transfer., Vol. 36, Pp. 618 – 623, 2009.

[8] I. Papautsky, B. Gale, S. Mohanty, T. Ameel, and B. Frazier, "Effects of Rectangular Microchannel Aspect Ratio on Laminar Friction Constant," Proceedings of SPIE, The Int.Society of Optical Engineering, Vol. 3877, Pp. 147-158, 1999.

[9] T.M. Harms, M.J. Kazmierczak, and F.M. Gerner, "Developing convective heat transfer in deep rectangular microchannels", Int. J. Heat Fluid Flow, Vol. 20, Pp. 149–157, 1999.

[10] J. Koo, and C. Kleinstreuer, "Laminar nanofluid flow in microheat-sinks", Int. J. Heat Mass Transfer., Vol. 48, Pp. 2652–2661, 2005.

[11] A. Kosar, "Effect of substrate thickness and material on heat transfer in microchannel heat sinks", Int. J. Therm. Sci., Vol. 49, Pp. 635–642, 2010.

[12] H.A. Mohammed, P. Gunnasegarana, and N.H. Shuaiba, "Heat transfer in rectangular microchannels heat sink using nanofluids", Int. Commun. Heat and Mass Transfer, Vol. 37, Pp. 1496-1503, 2010.

[13] F.M.A. Al-Dulaimy and G.Y.M. Al-Shahery, "Comparative simulation of different nanoparticles concentration using a rectangular heat transfer microchannel", Int. J. Nanoelectronics and Materials, Vol. 5, Pp. 101-116, 2012.

[14] P. Srivastava, A. Dewan, and J.K. Bajpai, "Flow and heat transfer characteristics in convergent-divergent shaped microchannel with ribs and cavities", International journal of heat and technology, Vol. 35, No. 4, Pp. 863-873, 2017.

[15] S. Mukherjee, P.C. Mishra, P. Chaudhuri, and G. Banerjee, "Theoretical modeling and optimization of microchannel heat sink cooling with TiO2-water and ZnO-water nanofluids", International Journal of Heat and Technology, Vol.36, No.1, Pp. 165-172, 2018.

[16] V. Saravanan, C.K. Umesh, D. Hithaish, and K. Seetharamu, "Numerical investigation of pressure drop and heat transfer in pin fin heat sink and micro channel pin fin heat sink", International Journal of Heat and Technology, Vol. 36, No. 1, Pp. 267-276, 2018.

[17] S. Mehrabi, S. Kheradmand, and O.R. Farivar, "Numerical simulation of thermal and hydraulic performance of a micro plate-pin fin heat sink", International Journal of Heat and Technology, Vol. 36, No. 3, Pp. 883-894, 2018.

[18] R.K. Ajeel, R.K. Ajeel, and K. Hasnan, "Numerical investigations of flow and heat transfer enhancement in a semicircle zigzag corrugated channel using nanofluids", International Journal of Heat and Technology, Vol. 36, No. 4, Pp. 1292-1303, 2018.

[19] C. Nguyen, F. Desgranges, G. Roy, N. Galanis, T. Maré, S. Boucher, and A.H. Mintsa, "Temperature and Particle-Size Dependent Viscosity Data for Water-Based Nanofluids - Hysteresis Phenomenon," Int. J. Heat Fluid Fl., Vol. 28, No. 6, Pp. 1492-1506, 2007.

[20] H.A. Mintsa, G. Roy, C.T. Nguyen, and D. Doucet, "New Temperature Dependent Thermal Conductivity Data for Water-Based Nanofluids," Int. J. Therm. Sci., Vol. 48, No. 2, Pp. 363-371, 2009.

[21] B. Vincenzo, N. Sergio, and M. Oronzio, "Enhancement of heat transfer and entropy generation analysis of nanofluids turbulent convection flow in square section tubes", Seconda Università degli Studi di Napoli, Via Roma 29, Aversa, CE 81031, Italy, Pp. 27, 2011.

[22] S.V. Patankar, "Numerical Heat Transfer and Fluid Flow", Hemisphere, New York, 1980.

[23] F.P. Incropera, D.P. Dewitt, T.L. Bergman, and A.S. Lavine, "Fundamentals of Heat and Mass Transfer", sixth ed. Wiley, New York, 2007.

NOMENCLATURE

Symbol	**Title**
f	Friction factor
k_f	Fluid thermal conductivity (W/m.K)
k_{nf}	Nanofluid thermal conductivity (W/m.K)
k_p	Particle thermal conductivity (W/m.K)
L_{ch}	Microchannel depth (m)
L_{hs}	Microchannel heat sink length (m)
$\dot{m}$	Mass flow rate (kg/s)
Nu	Nusselt number

Δp	Pressure drop across the microchannel (Pa)
q''	Heat flux (W/m^2)
Re	Reynolds number
T_s	Substrate (wafer) temperature (K)
u_m	Mean flow velocity (m/s)
$\dot{V}$	Coolant volumetric flow rate (m^3/s)
W	Width of the heat sink (m)
W_{ch}	Width of microchannel (m)
W_{fin}	Width of fin (m)
W_{hs}	Width of microchannel heat sink (m)

Greek Symbols

Symbol	**Title**
ρ	Density (kg/m^3)
μ	Viscosity ($N.s/m^2$)
φ	Volume fraction
v	Kinematic viscosity (m^2/s)

Abbreviation

Symbol	**Title**
CFD	Computational Fluid Dynamics
HTC	Heat Transfer Coefficient
MCHS	Microchannel heat sink
SIMPLE	Semi-Implicit Method for Pressure Linked Equation